Correspondence

Feature Band Selection for Online Multispectral Palmprint Recognition

Zhenhua Guo, David Zhang, Lei Zhang, and Wenhuang Liu

***Abstract*—A palmprint is a unique and reliable biometric feature with high usability. In the past decades, many palmprint recognition systems have been successfully developed. However, most of the previous work used the white light as the illumination source, and the recognition accuracy and anti-spoof capability is limited. Recently, multispectral imaging has attracted considerable research attention as it can acquire more discriminative information in a short time. One crucial step in developing online multispectral palmprint systems is how to determine the optimal number of spectral bands and select the most representative bands to build the system. This paper presents a study on feature band selection by analyzing hyperspectral palmprint data (520–1050 nm). Our experimental results showed that three spectral bands could provide most of the discriminate information of a palmprint. This finding could be used as the guidance for designing new online multispectral palmprint systems.**

***Index Terms*—Anti-spoof, biometrics, clustering, multispectral palmprint recognition.**

I. Introduction

Biometric authentication is the study of methods for recognizing humans based on one or more physical or behavioral traits [1]. As a unique biometric feature, palmprint recognition has attracted much attention in the past decade [2]–[5]. It owns many merits, such as high accuracy, high user-friendliness and low cost. However, there is substantial room to improve the palmprint systems, especially in the aspects of accuracy and its vulnerability to spoof attacks [6]. Multispectral imaging is an effective solution to such improvement [7].

Multispectral imaging could capture a series of palmprint images at various spectral bands simultaneously, recognition accuracy is improved as more discriminative information could be provided, and anti-spoof capability of systems is enhanced, because it is not a trivial issue to make a fake palm having the same spectral signatures with a real palm. Because of the advantages mentioned above, multispectral imaging has been not only applied on palmprint recognition [7]–[10], but also on other biometric systems, including multispectral fingerprint recognition [11], multispectral face recognition [12], [13], and multispectral iris recognition [14].

Manuscript received August 10, 2011; revised February 20, 2012; accepted February 22, 2012. Date of publication February 27, 2012; date of current version May 08, 2012. This work was supported in part by the GRF fund from the HKSAR Government, in part by the central fund from Hong Kong Polytechnic University, in part by the National Science Foundation of China (NSFC) under Grant 61101150 and Grant 61020106004, and in part by the China Postdoctoral Science Foundation under Grant 20100480301 and Grant 201104102. The associate editor coordinating the review of this manuscript and approving it for publication was Dr. Fabio Scotti.

Z. Guo and W. Liu are with the Graduate School at Shenzhen, Tsinghua University, Shenzhen, 518055, China (e-mail: zhenhua.guo@sz.tsinghua.edu.cn; liuwh@sz.tsinghua.edu.cn).

D. Zhang and L. Zhang are with the Department of Computing, Hong Kong Polytechnic University, Hong Kong, China (e-mail: csdzhang@comp.polyu.edu.hk; clzhang@comp.polyu.edu.hk).

Color versions of one or more of the figures in this paper are available online at http://ieeexplore.ieee.org.

Digital Object Identifier 10.1109/TIFS.2012.2189206

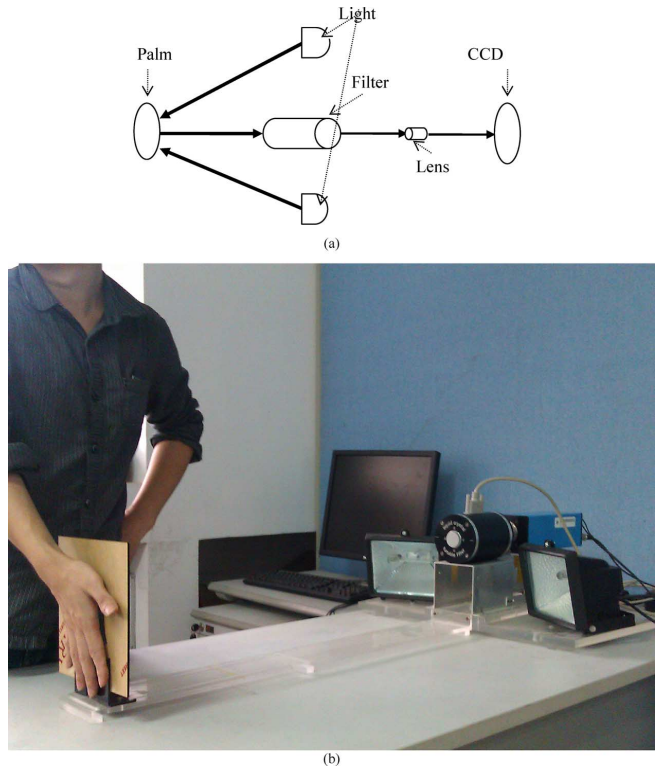

Fig. 1. Structure and prototype of hyperspectral palmprint imaging system. (a) Structure of the hyperspectral palmprint acquisition device. (b) Prototype of hyperspectral palmprint imaging system.

There are two underlying key issues which need to be addressed well before wide application of multispectral biometrics. First, how many spectra are enough for discriminating different palms? On one hand, usually more feature bands provide more information, thus higher accuracy could be expected. On the other hand, more feature bands require high cost on feature extraction and matching. Furthermore, due to the redundancy between different spectra, more information may fail to increase the accuracy sometimes [7], [10]. Second, how to choose representative spectra for a given number of feature bands? After determining the number of feature bands, a group of bands could be selected by some rules, such as divergence [12] and exhaustive searching [15]. The second issue belongs to feature selection [16], and some pioneering work has been made [12], [15]. However, to our best knowledge, there is no public report on the first issue for biometric research.

In this paper, we proposed a clustering-based method to determine the number of feature bands from a hyperspectral palmprint database. It is found that three spectral bands could contain most of the discriminant information. The finding is also validated by recognition experiments. In the following, Section II introduces the data collection of the hyperspectral palmprint cube. Section III reports the proposed spectral k-means clustering algorithm. Section IV shows the validation through verification experiments and Section V draws the conclusion.

II. Hyperspectral Palmprint Data Collection

To discover the optimal number of feature bands for multispectral palmprint recognition, a hyperspectral imaging system is established. The key components of the system include a liquid crystal tunable filter (LCTF) made by Meadowlark Inc., a charged coupled device (CCD)

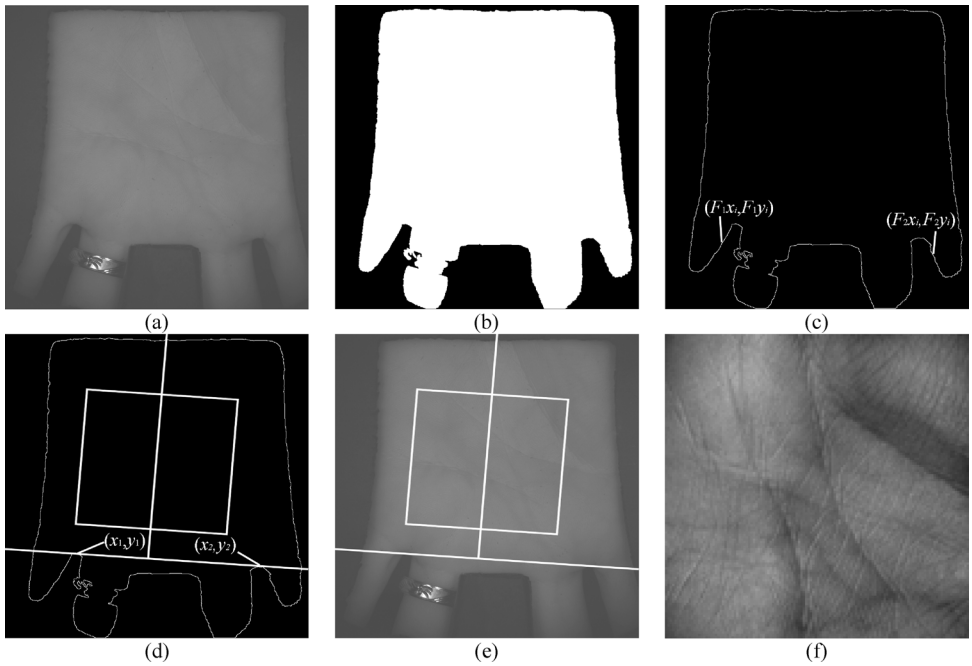

Fig. 2. Main steps of ROI extraction: (a) original image, (b) binary image, (c) boundary tracking, (d) building a coordinate system, (e) extracting the central part, and (f) ROI sample.

made by Cooke Corporation and two 500-W Osram halogen lights. The full width at half maximum (FWHM) of the filter is 5 nm when the center wavelength is 550 nm. A palm could be imaged at 69 spectral bands with a step-length of 10 nm over spectrum 420–1100 nm. Fig. 1 shows the imaging system.

After obtaining the hyperspectral cube, a local coordinate of the palmprint image is established in the center band (760 nm), and then a region of interest (ROI) is cropped from each band based on the local coordinate. The ROI extraction includes five steps [7]: 1) convert original image to a binary image; 2) obtain the boundaries of two gaps, $(F_j x_i, F_j y_i)$ $(j = 1, 2)$ between the fingers; 3) compute the tangent line of the two gaps where (x_1, y_1) and (x_2, y_2) are two intersect points with the tangent line; 4) line up (x_1, y_1) and (x_2, y_2) to get the Y-axis, and use the perpendicular bisector of Y-axis as X-axis; 5) extract a fixed size subimage based on the coordinate. Fig. 2 illustrates the main steps to extract the ROI.

Fig. 3 shows the ROI samples in different spectra. As shown in Fig. 3, in the visible spectrum, palm lines are very clear and palm veins are hard to be found; while in the near infrared (NIR) spectrum, palm veins become clear and palm lines are weak. In this study, palm veins are regarded as a kind of special palmprint feature, dark palm lines. Thus, a typical palmprint recognition method is used here. How to fully utilize the vein pattern by NIR illumination is out of focus of this study and thus it will be our future work. For the convenience of analysis, these ROIs are normalized to a size of $128 * 128$. To reduce the intensity effect, the ROIs are converted to have a mean intensity of 128 with a standard deviation of 20. The first ten and the last five spectra are removed due to the low quality of images [15]. Thus, in the following, only 54 feature bands (520–1050 nm, with 10-nm intervals) are used.

A large hyperspectral palmprint database from 190 individuals was built. The subjects were mainly volunteers from our institutes. In the database, the age distribution was from 20 to 60 years old. The hyperspectral palmprint cubes were collected by two separate sessions. The average time interval between the two occasions was around 1 month. In each session, the subject was asked to provide around seven cubes of each of his/her left and right palms, so the database contains 5240 images for each band from 380 different palms. Among them, 2608 cubes were collected in the first session, while 2632 in the second session.

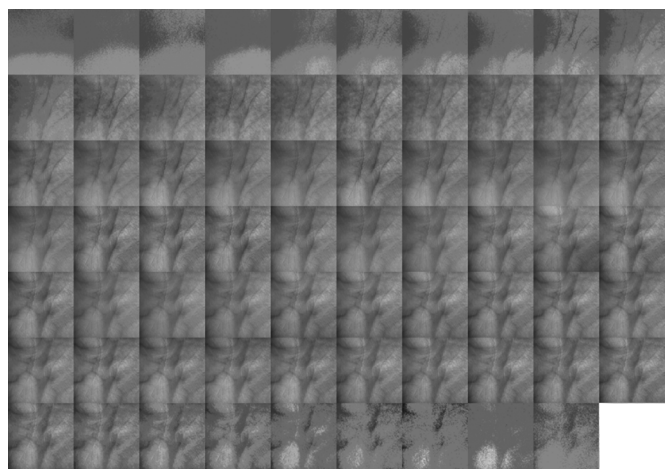

Fig. 3. ROIs extracted from a hyperspectral palmprint cube sample. From left to right, from top down, wavelength is increasing from 420 to 1100 nm with 10-nm intervals.

III. Feature Band Selection by Clustering

A. Review of k-Means

The k-means clustering algorithm [16] is a basic and well-known technique in pattern recognition. During the clustering, some points are clustered into separated classes or clusters according to the given clustering criterion.

As k is a critical input parameter, different values will generate different clustering results. When the k is smaller or equal to the true number of clusters, the center distance is very big; while the k is larger than the true number of clusters, one cluster will be split into small

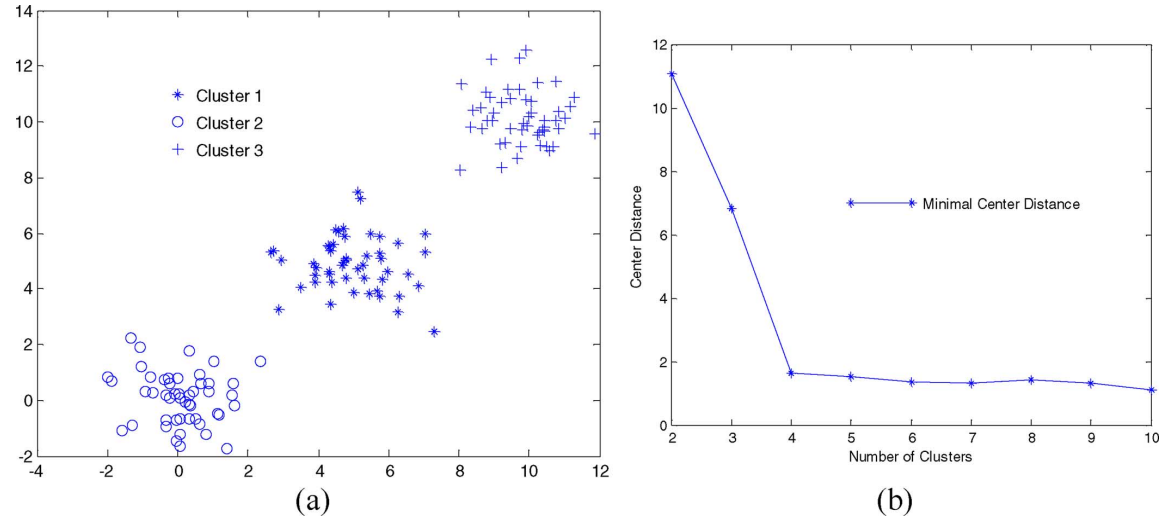

Fig. 4. (a) Original data. (b) Number of clusters versus minimal center distance.

clusters, the center distance becomes smaller and stable. The minimal center distance is defined as

$$d^k_{\min} = \min_{\substack{1\le i\le k\\ 1\le j\le k\\ i\neq j}} (d_{i,j}) \tag{1}$$

$$d_{i,j} = d(c_i, c_j) \tag{2}$$

where d is Euclidean distance, c is the cluster center and k is the number of clusters.

Fig. 4 shows an example of k-means and its $d^k_{\min}$. Fig. 4(a) shows three clusters which are generated by three separate Gaussian distributions, while Fig. 4(b) shows the $d^k_{\min}$ for different k values. As illustrated by Fig. 4(b), the distance drops quickly from $k = 2$ to $k = 3$. When k is bigger than 3, the distance changes slowly. This example shows that k-mean clustering could be used to discover the true number of clusters. Based on this finding, a spectral k-means clustering algorithm is proposed.

B. Introduction of Complex Wavelet Structural Similarity (CW-SSIM) Distance

Suppose there is a mother wavelet $w(u) = g(u)e^{j\omega_c u}$, where ω_c is the center frequency of the modulated bandpass filter and $g(u)$ is a slowly varying and symmetric function. The family of wavelets are dilated and translated versions of $w(u)$

$$w_{s,p}(u) = \frac{1}{\sqrt{s}} w\left(\frac{u-p}{s}\right) = \frac{1}{\sqrt{s}} g\left(\frac{u-p}{s}\right) e^{j\omega_c(u-p)/s} \tag{3}$$

where scale factor $s \in R^+$ and translation factor $p \in R$. The continuous complex wavelet transform of a given real signal $x(u)$ is [25]

$$X(s,p) = \frac{1}{2\pi} \int_{-\infty}^{\infty} X(\omega) \sqrt{s}\, G(s\omega - \omega_c)\, e^{j\omega p} d\omega \tag{4}$$

where $X(\omega)$ and $G(\omega)$ are the Fourier transforms of $x(u)$ and $g(u)$, respectively. The discrete wavelet coefficients are sampled versions of the continuous wavelet transform.

To compute the CW-SSIM similarity of two images, we first compute the complex wavelet transform of them. Denote by $\mathbf{c}_x = \{c_{x,i} | i = 1, 2, \ldots I\}$ and $\mathbf{c}_y = \{c_{y,i} | i = 1, 2, \ldots I\}$ the complex wavelet coefficients of the two images. The CW-SSIM similarity of $\mathbf{c}_x$ and $\mathbf{c}_y$ is computed as

$$\tilde{S}_m(\mathbf{c}_x, \mathbf{c}_y) = \frac{\left|\sum_{i=1}^{I} c_{x,i} c^*_{y,i}\right| + K}{\sum_{i=1}^{I} |c_{x,i}||c_{y,i}| + K}. \tag{5}$$

Here, c^* denotes the complex conjugate of c and K is a small positive constant. $\tilde{S}_m(\mathbf{c}_x, \mathbf{c}_y)$ is fully determined by the consistency of phase changes between $\mathbf{c}_x$ and $\mathbf{c}_y$. It has been shown that the CW-SSIM similarity is insensitive to luminance and contrast changes as well as small translation, rotation and distortion. It achieves the maximum value 1 only when the two images have the same structure [17]. The overall similarity of the two palmprint images, denoted by s, can be estimated as the average of CW-SSIM $\tilde{S}_m$ across M (M is defined as 6 here) orientations. Finally, the CS-SSIM distance is computed by $d = 1 - s$.

C. Proposed Spectral k-Means Clustering

Suppose we have N hyperspectral palmprint cubes with B spectra as the training set, Fig. 5 shows the pseudo-code of the algorithm where $N = 2280$ ($380 * 6$, the first 6 cubes of each palm were selected), $B = 54$ and $T = 100$.

Because there is the possibility that the clustering ends at local minimal instead of global minimal, for a given k, the clustering runs 1000 times and the most frequent cluster centers are kept as the final result for the given k. Fig. 6 shows the minimal center distance for different numbers of clusters.

Fig. 6 shows that three clusters may be enough to represent the 54 feature bands. The $k = 3$ cluster result is listed in Table I and the distance map between different wavelengths is plotted in Fig. 7. As it can be seen from Fig. 7, there are roughly three dark blocks. According to the spectrum definition [19], the three clusters could be roughly named as visible spectrum without red, red spectrum and NIR spectrum.

IV. Clustering Validation by Verification Test

To demonstrate whether three is the optimal number of feature bands, verification experiments are implemented to validate it. Here,

1. Randomly get k initialized centers (wavelengths), x=0;
2. For any wavelength j (j=1,2,…,B), compute the distance between the wavelength with k centers, here the distance is compute as:

$$D_{i,j} = \sum_{n=1}^{N} d_{i,j}^{n} = \sum_{n=1}^{N} d^{n}(c_i, w_j), i = 1,2,...,k$$

where c is the centre wavelength, w_j is the given wavelength, and d is the CW-SSIM distance defined above.

x=x+1;

3. For each centre, find the wavelengths which have the minimal distance among n centres. There are k clusters of wavelengths:

$$S_i = \{j \mid \arg\min_i D_{i,j} = i\}, i = 1,2,...,k$$

4. For any cluster, find the wavelength which has the minimal average distance with the remaining wavelengths in the cluster, this wavelength is updated as the new center:

$$c_i^{'} = \arg\min_{m \in S_i} \sum_{l=1}^{B} D_{l,m}, l \neq m, l \in S_i$$

5. If the centres are not changed or x=T (T is a predefined iteration threshold), stops; otherwise, goes to step 2.

Fig. 5. Pseudo-code of proposed spectral k-means clustering.

TABLE I
CLUSTERING RESULT OF SPECTRAL k-MEAN FOR $k = 3$

Cluster	Wavelengths
1	520 530 540 550 560 570 580 590 600 610
2	620 630 640 650 660 670 680 690 700 710 720 730 740 750 760 770 780
3	790 800 810 820 830 840 850 860 870 880 890 900 910 920 930 940 950 960 970 980 990 1000 1010 1020 1030 1040 1050

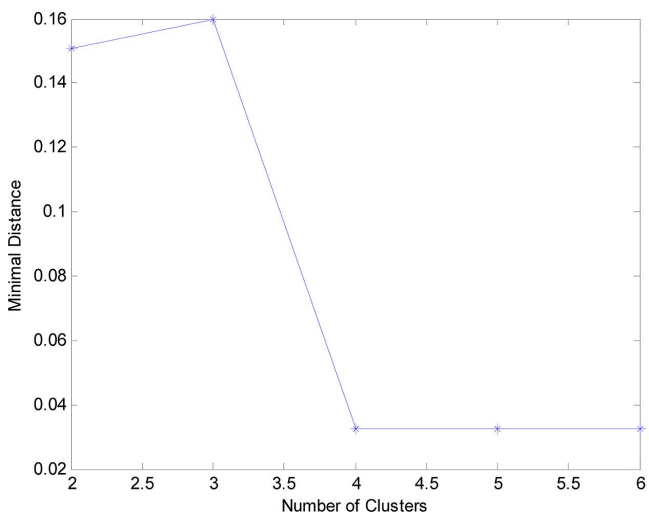

Fig. 6. Minimal distance of spectral versus k.

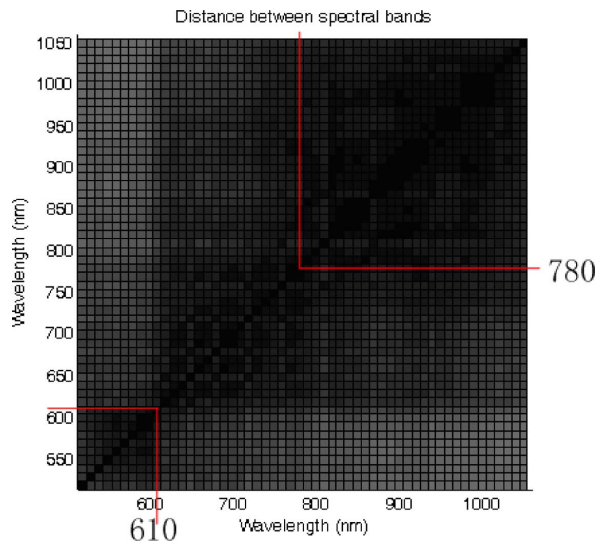

Fig. 7. Distance map between different feature bands. Distance is converted from [0, 1] to [0, 255] for display.

CW-SSIM distance is selected as the metric for verification test as it is less sensitive to scale, rotation and translation variation for palmprint verification [17], [18].

One cube of each palm in the first session is randomly selected as the gallery sample, thus totally 380 gallery images are selected for one feature band; all the cubes in the second session are used as probe samples, and totally 2632 probe images for each feature band are used. For any feature band, the CW-SSIM distance between each sample in the gallery set and each sample in the probe set is computed. The distance is 0 only when the two images are identical. Totally, there are 1 000 160 ($380 * 2632$) CW-SSIM distances for each feature band. A match is counted as genuine if the two palmprint images are from the same palm; otherwise, the match is counted as an impostor. Among them, 2632 distances are genuine matching distances while the remaining are impostor matching distances. Equal error rate [(EER) when false acceptance rate (FAR) equals to false rejection rate (FRR)] is used to evaluate the accuracy [7]. To get unbiased results with the training gallery selection, the gallery set is selected three times independently.

Then, one cube of each palm in the second session is randomly selected as the gallery sample, therefore, totally 380 gallery images are selected for one feature band; and all the cubes in the first session are used as probe samples, so in total 2608 probe images for each feature band are used. We use the same test protocol for each wavelength, and get 991 040 ($380 * 2608$) matching distances for each feature band. Among them, 2608 distances are genuine matching distances while

TABLE II
FUSION RESULTS FOR DIFFERENT NUMBER OF FEATURE BANDS

Number of feature bands	Optimal Combination	EER (%) (Mean±Standard deviation)
1	790nm	0.2220±0.0652
2	580nm, 770nm	0.1039±0.0431
3	580nm, 760nm, 990nm	0.0780±0.0344
4	580nm, 620nm, 760nm ,940nm	0.0727±0.0430

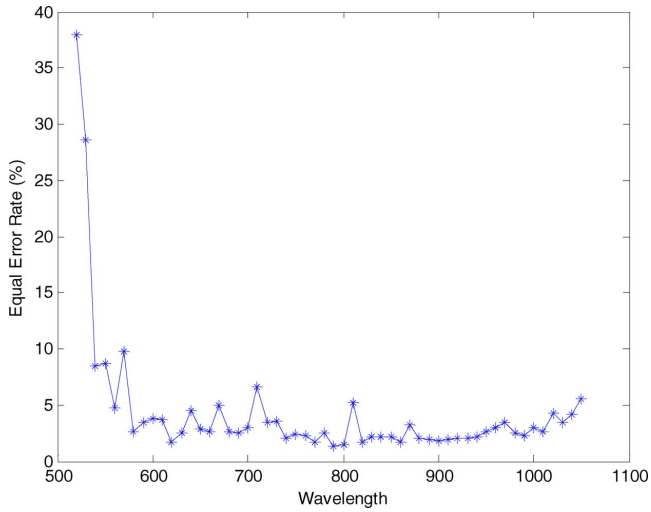

Fig. 8. Wavelength versus EER.

the remaining are impostor matching distances. Similarly, the gallery set is selected three times independently. Thus, in total six verification trials are implemented. In the following, the average EER of the six trials is listed as experimental results. Fig. 8 illustrates the EER with different wavelengths. The lowest EER is achieved by 790 nm with EER $= 0.2220\%$.

To find the optimal combination for a given number of feature bands, many algorithms could be used to search for the combination, such as divergence [20], mutual information [21], and entropy [22]. Here, an exhaustive search is implemented as it will find the optimal combination for the given dataset. Sum score level fusion [23] is used as the fusion technique on the dataset. The lowest EER for each combination is listed in Table II.

Table II shows that more feature bands corresponds to higher accuracy. For example, the fusion of two bands could reduce the EER from 0.222% to 0.1039%. However, the improvement from three bands to four bands is very small. It is only 0.0053%. Using statistical analysis [24], the difference between the fusion of four bands and three bands is not statistically significant. And as shown in Table I, 580 nm, 760 nm, and 990 nm come from three different clusters. These findings are consistent with the results obtained in the previous section: three spectra are enough for a palmprint. This is mainly because that human skin is made up of three layers: the epidermis, dermis, and subcutis, as shown in Fig. 9. Each layer contains a different proportion of blood and fat. The epidermis also contains melanin, while the subcutis contains veins [26]. Different light wavelengths will penetrate different skin layers and illuminate in different spectra. Thus, visible spectrum without red (580 nm), red spectrum (760 nm) and NIR (990 nm) spectrum could enhance different layers of palm and contain most of useful features for palmprint verification.

Fig. 10 shows a multispectral palmprint example. As shown in Fig. 10, a 580-nm palmprint image contains clear palm line information only, and a 760-nm palmprint image has palm lines and weak

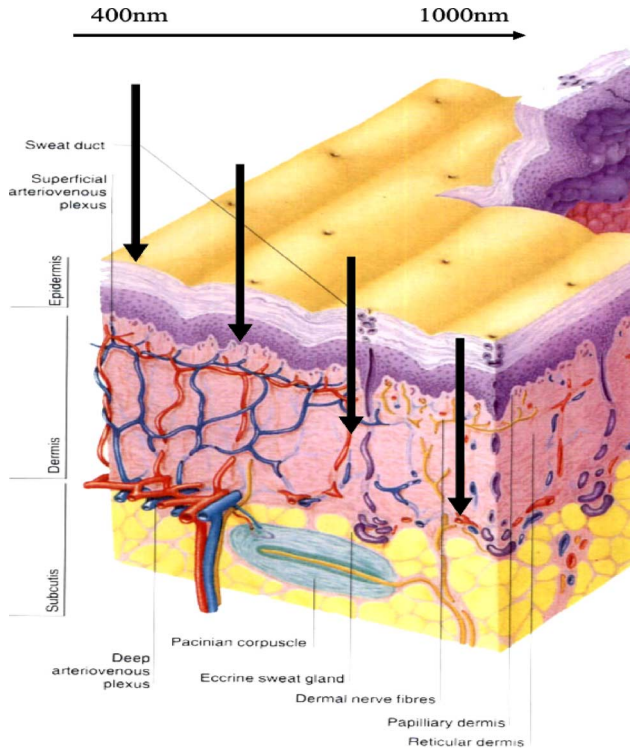

Fig. 9. Cross-section anatomy of the skin [7].

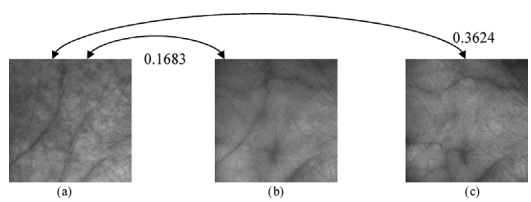

Fig. 10. Multispectral palmprint sample. (a)–(c) Three palmprint images of a true palm. CS-SSIM distance between two images is shown on or near a double arrow curve. (a) 580 nm. (b) 760 nm. (c) 990 nm.

palm veins, while a 990-nm palmprint image could get clear palm veins and weak palm lines. Since different palmprint image under different wavelengths could enhance different skin layers and features, with the increase of the wavelength difference, the CS-SSIM distance illustrated in Fig. 10 increases. Because it is difficult to make a fake palm with complicated skin layers, the faked palmprint images under different wavelengths are very similar [7]. Thus, liveness detection could be applied by analyzing the distances between different wavelengths.

V. CONCLUSION

In this paper, a spectral k-means clustering algorithm is proposed to cluster hyperspectral palmprint cubes. The clustering could be used to determine an optimal number of feature bands. The result shows that

three feature bands may be enough to represent the palmprint features. Based on score level fusion and exhaustive searching on all fusion candidates, three feature bands could get much better results than two bands and it can get comparable results with four bands. This finding validates the effectiveness of the proposed clustering algorithm and it is empirically demonstrated that three feature bands is a good option for real multispectral palmprint applications. In the future, a new online multispectral palmprint system will be designed based on the findings in this paper.

However, the hyperspectral database is limited to Chinese persons only. Whether the finding is applicable to other groups needs further investigation. In this study, the palm vein is regarded as a kind of special palmprint feature, dark palm line, thus, a typical palmprint recognition method is used. Another research direction is how to fully utilize the vein pattern in NIR illumination [27].

REFERENCES

[1] A. Jain, R. Bolle, and S. Pankanti, Eds., Biometrics: Personal Identification in Network Society. Boston, MA, Kluwer Academic, 1999.

[2] T. Connie, T. Andrew, and K. Goh, "An automated palmprint recognition system," *Image Vision Computing*, vol. 23, pp. 501–505, 2005.

[3] D. Hu, G. Feng, and Z. Zhou, "Two-dimensional locality preserving projections (2DLPP) with its application to palmprint recognition," *Pattern Recognition*, vol. 40, pp. 339–342, 2007.

[4] C. Han, H. Cheng, C. Lin, and K. Fan, "Personal authentication using palm-print features," *Pattern Recognition*, vol. 36, pp. 371–381, 2003.

[5] W. Jia, D. Huang, and D. Zhang, "Palmprint verification based on robust line orientation code," *Pattern Recognition*, vol. 41, pp. 1504–1513, 2008.

[6] S. A. C. Schukers, "Spoofing and anti-spoofing measures," *Inform. Security Tech. Rep.*, vol. 7, pp. 56–62, 2002.

[7] D. Zhang, Z. Guo, G. Lu, L. Zhang, and W. Zuo, "An online system of multi-spectral palmprint verification," *IEEE Trans. Instrumentation Measurement*, vol. 59, no. 3, pp. 480–490, Mar. 2010.

[8] Y. Hao, Z. Sun, and T. Tan, "Comparative studies on multispectral palm image fusion for biometrics," in *Proc. Asian Conf. Computer Vision*, 2007, pp. 12–21.

[9] R. K. Rowe, U. Uludag, M. Demirkus, S. Parthasaradhi, and A. K. Jain, "A Multispectral whole-hand biometric authentication system," in *Proc. Biometric Symp., Biometric Consortium Conf.*, 2007, pp. 1–6.

[10] Y. Hao, Z. Sun, T. Tan, and C. Ren, "Multispectral palm image fusion for accurate contact-free palmprint recognition," in *Proc. Int. Conf. Image Processing*, 2008, pp. 281–284.

[11] R. K. Rowe, K. A. Nixon, and S. P. Corcoran, "Multi spectral fingerprint biometrics," in *Proc. Information Assurance Workshop*, 2005, pp. 14–20.

[12] H. Chang, Y. Yao, A. Koschan, B. Abidi, and M. Abidi, "Improving face recognition via narrowband spectral range selection using Jeffrey divergence," *IEEE Trans. Inform. Forensics Security*, vol. 4, no. 1, pp. 111–122, Feb. 2009.

[13] W. Di, L. Zhang, D. Zhang, and Q. Pan, "Studies on hyperspectral face recognition in visible spectrum with feature band selection," *IEEE Trans. Systems, Man, Cybernetics—Part A: Syst. Humans*, vol. 40, no. 6, pp. 1354–1361, Dec. 2010.

[14] C. Boyce, A. Ross, M. Monaco, L. Hornak, and X. Li, "Multispectral iris analysis: A preliminary study," in *Proc. IEEE Computer Society Conf. Computer Vision and Pattern Recognition, Workshops*, 2006, pp. 51–59.

[15] Z. Guo, L. Zhang, and D. Zhang, "Feature band selection for multispectral palmprint recognition," in *Proc. Int. Conf. Pattern Recognition*, 2010, pp. 1136–1139.

[16] R. O. Duda, P. E. Hart, and D. G. Stork, *Pattern Classification*. New York: Wiley, 2001.

[17] L. Zhang, Z. Guo, Z. Wang, and D. Zhang, "Palmprint verification using complex wavelet transform," in *Proc. Int. Conf. Image Processing*, 2007, pp. 417–420.

[18] M. P. Sampat, Z. Wang, S. Gupta, A. C. Bovik, and M. K. Markey, "Complex wavelet structural similarity: A new image similarity index," *IEEE Trans. Image Process.*, vol. 18, no. 10, pp. 2385–2401, Oct. 2009.

[19] Visible Spectrum Wikipedia [Online]. Available: http://en.wikipedia.org/wiki/Visible_spectrum

[20] H. Chang, Y. Yao, A. Koschan, B. Abidi, and M. Abidi, "Spectral range selection for face recognition under various illuminations," in *Proc. Int. Conf. Image Processing*, 2008, pp. 2756–2759.

[21] B. Guo, S. R. Gunn, R. I. Damper, and J. D. B. Nelson, "Band selection for hyperspectral image classification using mutual information," *IEEE Geosci. Remote Sensing Lett.*, vol. 3, no. 2, pp. 522–526, Apr. 2006.

[22] H. Wang and E. Angelopoulou, "Sensor band selection for multispectral imaging via average normalized information," *J. Real-Time Image Processing*, vol. 1, pp. 109–121, 2006.

[23] A. A. Ross, K. Nadakumar, and A. K. Jain, *Handbook of Multibiometrics*. New York: Springer, 2006.

[24] W. Mendenhall, R. J. Beaver, and B. M. Beaver, *Introduction to Probability and Statistics*, 13th ed. Belmont, U.S.: Brooks/Cole, Cengage Learning, 2009.

[25] Z. Wang and E. P. Simoncelli, "Local phase coherence and the perception of blur," in *Adv. Neural Information Processing Systems (NIPS03)*, Cambridge, MA, May 2004, vol. 16.

[26] D. J. Gawkrodger, *Dermatology: An Illustrated Colour Text*, 3rd ed. New York: Elsevier Health Sciences, 2002.

[27] J.-G. Wang, W.-Y. Yau, A. Suwandy, and E. Sung, "Person recognition by fusing palmprint and palm vein images based on "Laplacianpalm" representation," *Pattern Recognition*, vol. 41, no. 5, pp. 1514–1527, 2008.